Bulletin of the Seismological Society of America, Vol. 76, No. 6, pp. 1614–1622, December 1986

INTERPLATE COUPLING AND TEMPORAL VARIATION OF MECHANISMS OF INTERMEDIATE-DEPTH EARTHQUAKES IN CHILE

By Luciana Astiz and Hiroo Kanamori

Abstract

We investigated the temporal variation of the mechanism of large intraplate earthquakes at intermediate depths in relation to the occurrence of large underthrusting earthquakes in Chile. Focal mechanisms were determined for three large events (1 March 1934: $M = 7.1$, $d = 120$ km; 20 April 1949: $M = 7.3$, $d = 70$ km; and 8 May 1971: $M_W = 7.2$, $d = 150$ km) which occurred down-dip of the great 1960 Chilean earthquake ($M_W = 9.5$) rupture zone. The 1971 event is down-dip compressional: θ (strike) = 12°, δ (dip) = 80°, and λ (rake) = 100°. The 1949 earthquake focal mechanism is $\theta = 350°$, $\delta = 70°$, and $\lambda = -130°$. The data available for the 1934 event are consistent with a down-dip tensional mechanism. Thus, the two events which occurred prior to the great 1960 Chilean earthquake are down-dip tensional. Published fault plane solutions of large intermediate-depth earthquakes (28 March 1965 and 7 November 1981) which occurred down-dip of the Valparaiso earthquakes of 1971 ($M_W = 7.8$) and 1985 ($M_W = 8.0$) are also down-dip tensional. These results suggest that before a major thrust earthquake, the interplate boundary is strongly coupled, and the subducted slab is under tension at intermediate depths; after the occurrence of an interplate thrust event, the displacement on the thrust boundary induces transient compressional stress at intermediate depth in the down-going slab. This interpretation is consistent with the hypothesis that temporal variations of focal mechanisms of outer-rise events are due to changes of interplate coupling.

Introduction

The mechanism of intraplate earthquakes has been often used to infer the state of stress in the lithosphere. Isacks and Molnar (1971) interpreted the intraplate stress orientations in terms of spatial variations of the geometry of the Benioff zone. Double seismic zones which are most clearly defined for the Japanese subduction zone (Hasegawa *et al.*, 1978) have been related to the state of stress in the subducting slab (e.g., Sleep, 1979; Kawakatsu, 1986) Seno and Pongswat (1981) and Kawakatsu and Seno (1981) found a third seismic zone in northern Japan, and suggested that the focal mechanism of the events in this zone changes in response to stress changes on the interplate thrust boundary. Fujita and Kanamori (1981) examined published mechanism solutions for intermediate-depth earthquakes and interpreted the result in terms of the global variation of interplate coupling on the subduction-zone thrust plane.

Christensen and Ruff (1983) suggested that the stress axes of outer-rise earthquakes are closely related to the spatiotemporal variation of activity of interplate thrust earthquakes. They found only tensional outer-rise events for uncoupled subduction zones, and suggested that the slab is under tension due to the slab pull. For coupled seismic zones, they observed a temporal variation of the stress orientation of outer-rise events associated with the occurrence of large underthrusting earthquakes. Although most shallow outer-rise events are tensional (normal fault), compressional (thrust) events occur offshore of some seismic gaps. They hypothesized that, for strongly coupled subduction zones, the intraplate stress orientation in the outer-rise region is compressional before a large interplate thrust earthquake;

after the occurrence of a large thrust earthquake, the interplate boundary is temporarily uncoupled, and the stress becomes tensional.

Astiz *et al.* (1984) found that most large ($M > 6.8$) intermediate-depth earthquakes occurring down-dip of strongly coupled subduction zones have a steeply dipping normal-fault mechanism that is consistent with down-dip tensional stresses within the subduction plate (Figure 1). As a possible interpretation of this observation, they suggested that, at strongly coupled subduction zones, the stresses caused by the negative buoyancy of the subducting slab tends to cause (down-dip tensional) normal-fault earthquakes in the downgoing slab near the lower edge of the coupled thrust plane. These results suggest that intraplate stress reflects the degree of coupling at the interplate thrust boundary. Here, we define strong and weak seismic coupling in terms of the occurrence and absence of great ($M > 8.5$) subduction events.

In contrast with most South American intermediate-depth events which are down-dip tensional (Baranzangi and Isacks, 1976), the mechanism of the 8 May 1971 ($M_S = 6.8$) earthquake is down-dip compressional. This is the only event with $M > 6.5$ to have occurred after the 1960 Chilean ($M_W = 9.5$) earthquake down-dip of its rupture zone. This contrast in the stress orientation may be a result of the large interplate displacement associated with the 1960 Chilean earthquake. To investigate this problem, we examined spatiotemporal variations of large intermediate-depth earthquakes along the Chilean subduction zone.

Seismicity in Southern Chile

The shallow seismicity in the Chilean subduction zone dips gently (10°), bending at intermediate depths (to 25°) and extending to about 200 km depth (Barazangi and Isacks, 1976). Figure 2 shows the rupture zones of the recent shallow large earthquakes that occurred in southern Chile (6 April 1943, $M_t = 8.2$; 9 July 1971, $M_W = 7.8$; 3 March 1985, $M_W = 8.0$; 1 December 1928, $M_t = 7.9$; 25 January 1939, $M_t = 8.3$; and 21 May 1960, $M_W = 9.5$. Here, M_W is the moment magnitude and M_t is the tsunami magnitude. The 1960 Chilean earthquake is the largest in this

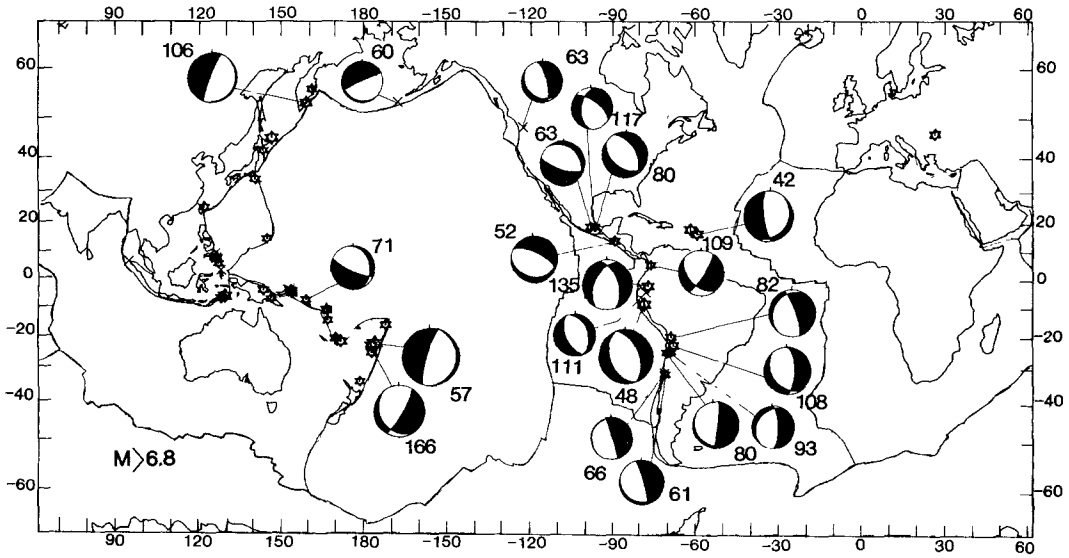

FIG. 1. The mechanisms (compression quadrants, darkened) of large ($M > 6.8$) intermediate-depth "normal-fault" earthquakes for the period 1960 to 1984. Numbers indicate the focal depth.

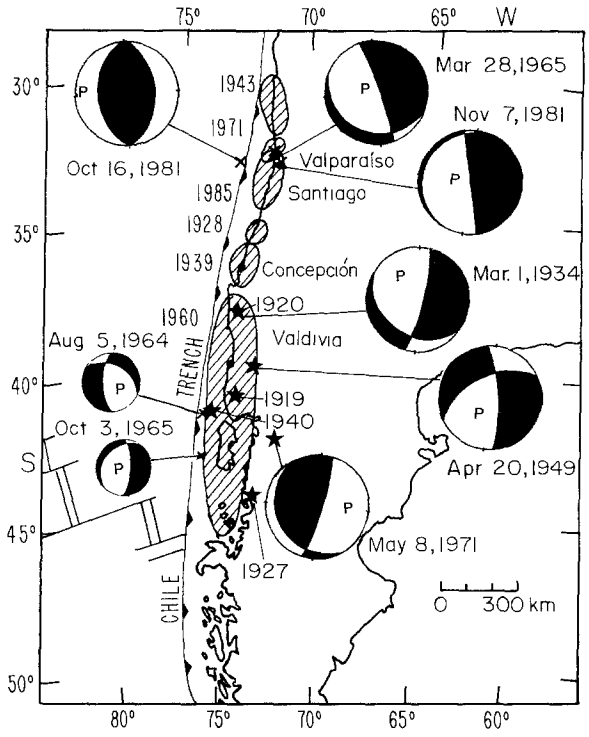

FIG. 2. The rupture areas of the recent large shallow earthquakes in central and southern Chile (Kelleher, 1972; Korrat and Madariaga, 1986). The epicenters of large ($M > 7.5$) earthquakes which occurred before the 1960 Chile earthquake, south of 37°S, are indicated (Table 1). Fault plane solutions of large ($M \geqq 7.0$) intermediate-depth earthquakes which occurred from 1930 to 1985 and the solutions for the 1964, 1965, and 1981 outer-rise events are also shown. Note that the events occurring before the 1960 Chile earthquake and also those occurring before the 1971 and 1985 Valparaiso earthquakes at intermediate depths are steeply dipping faults (down-dip tensional). In contrast, the 8 May 1971 event that occurred after the 1960 earthquake is down-dip compressional.

century, involving extensive crustal deformation (Plafker and Savage, 1970) and accounting for most of the convergence along the plate boundary (Kanamori and Cipar, 1974). The subduction zone along the rupture zone of the 1960 Chilean earthquake is associated with a young subducting slab and large convergence rate. Ruff and Kanamori (1983) point out that these features are usually associated with strong interplate coupling.

The 8 May 1971 earthquake is the only large event which occurred down-dip of the rupture zone of the 1960 great Chilean earthquake during the period from 1961 to 1985. We searched for possible large intermediate-depth events that may have occurred during the aftershock sequence of the 1960 Chilean earthquake. Duda (1963) assigns intermediate depths to some of the large 1960 Chilean aftershocks. However, comparing Duda's hypocenters with the International Seismological Centre (ISC) and National Oceanic and Atmospheric Administration (NOAA) hypocentral locations, we found that all of these events are listed as shallow (<40 km). The largest of these events (1 November 1960, $M_S = 7.2$) is a shallow complex event (Kanamori and Stewart, 1979).

We searched for all large earthquakes which occurred before 21 May 1960 between 37° and 47°S in Chile (shown by stars in Figure 2, Table 1). The 1919 doublet, and the 1920, 1927, and 1940 earthquakes are listed as large shallow earthquakes; however, the *ISC Bulletin* indicates that the 1919 doublet may be as deep as 130

TABLE 1

LARGE EARTHQUAKES IN SOUTHERN CHILE BEFORE 1960*

Date	Time	Latitude (°S)	Longitude (°W)	Depth (km)	M_S
2 Mar. 1919	3h 26m	41.0	73.5	40	7.2
2 Mar. 1919	11h 45m	41.0	73.5	40	7.3
10 Dec. 1920	4h 25m	39.0	73.0		7.4
21 Nov. 1927	23h 12m	44.3	73.0		7.1
1 Mar. 1934	21h 45m	40.0	73.0	120	7.1
11 Oct. 1940	18h 41m	41.5	74.5		7.0
20 Apr. 1949	3h 29m	38.0	73.5	70	7.3

* Hypocenters are taken from Gutenberg and Richter (1954).

km. We could not find any records or first motion data for the events prior to 1930; consequently, we could not analyze these events. For the 1940 earthquake, ISC first motion data are consistent with a shallow (15°) dipping thrust fault, with a strike subparallel to the trench axis (350°) in southern Chile; it probably occurred on the interplate boundary. However, the location of this event (41.5°S, 74.5°W) given by Gutenberg and Richter (1954) is very close to the trench axis (Figure 2). If this location is correct, this event could be an outer-rise event with a horizontal compression mechanism. Unfortunately, the data are not good enough to resolve the location and nature of this event. For the 1949 and 1934 earthquakes, we have a few seismograms and also *P*-wave first motion data reported by ISC. Using these seismograms, we determined orientations of the stress axes with respect to the down-going plate. In the following, we describe our mechanism solutions.

DATA ANALYSIS

Since the data for old events are incomplete, we combine *P*-wave first motion data, *S*-wave polarization angles and waveform data to determine the mechanisms. We use synthetic seismograms to interpret the observed waveforms. All synthetic seismograms are computed using the method described by Langston and Helmberger (1975). We assume a half-space with $V_p = 7.3$ km/sec, $V_s = 4.1$ km/sec, and $\rho = 3.1$ gm/cm^3 to determine the source depth, orientation, and the source time function. *P*-wave records are from vertical component recordings and *SH*-wave records are obtained by rotating the observed horizontal seismograms. *SH* clockwise motions around the source viewed from above are shown as upward motions (Figures 3 to 5). Note that for intermediate-depth earthquakes, the arrival times of the reflected phases relative to the direct phase provide good constraints on the focal depth, and there is no trade-off between the source time function and the depth of the events. Although the absolute amplitude of near nodal phases may be difficult to match between the observed and calculated records due to this simplified structure, the relative amplitude between the direct and reflected phases can be used to determine the focal mechanism. Note that stations that are far from the node of the direct *P* arrival can be near nodal for the surface reflected phases.

The 1971 earthquake. Figure 3 shows the first motion data obtained from short- and long-period vertical seismograms of most WWSSN stations. These data constrain the steeply dipping fault plane. We modeled long-period *P* and *SH* waveforms (upper traces) for Pasadena ($T_0 = 1$ sec, $T_g = 90$ sec) and WWSSN stations distributed over a large azimuthal range. Note that North American stations (WES, GEO, JCT, and PAS) are near-nodal for the *pP* arrival. The fault parameters determined are θ (strike) = 12°, δ (dip) = 80°, and λ (rake) = 100°. Synthetic

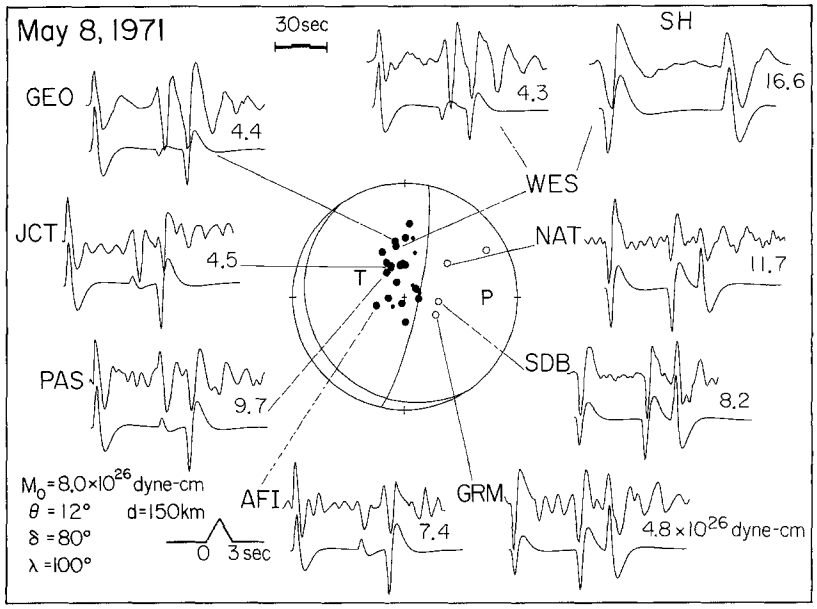

FIG. 3. Observed (*upper trace*) and synthetic (*lower trace*) *P* and *SH* waveforms for the 8 May 1971 earthquake. The best-fitting synthetics are for a source 150 km deep and 3 sec long. The number given to each seismogram is the seismic moment determined from that record.

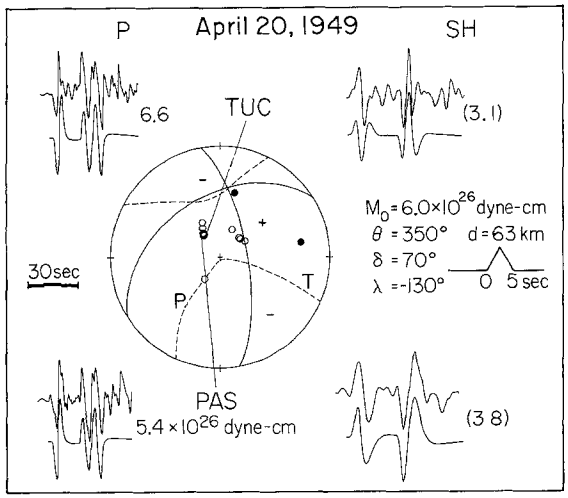

FIG. 4. Reported first motion data for the 20 April 1949 earthquake from the *ISC Bulletin*. Dashed lines are the *SH*-wave radiation node; + indicates clockwise rotation around the source when seen from above. The *upper traces* are *P* and *SH* waveforms recorded at Pasadena and Tucson. The *lower traces* are synthetic seismograms for a steeply dipping normal fault: $\theta = 350°$, $\delta = 70°$ and $\lambda = -130°$.

seismograms constrained the azimuth of the low-angle plane to within 10°. The source time function is 3 sec long, and the depth is 150 km. The seismic moment determined for each station is given in Figure 3. The average seismic moment obtained from *P* waves alone is 8.0×10^{26} dyne-cm ($M_W = 7.2$).

The 1949 event. First motion data for this event reported by teleseismic stations in the *ISC Bulletin* indicate that the tension axis is parallel to the slab dip (Figure 4). *P* waveforms were digitized from Benioff vertical long-period seismograms at

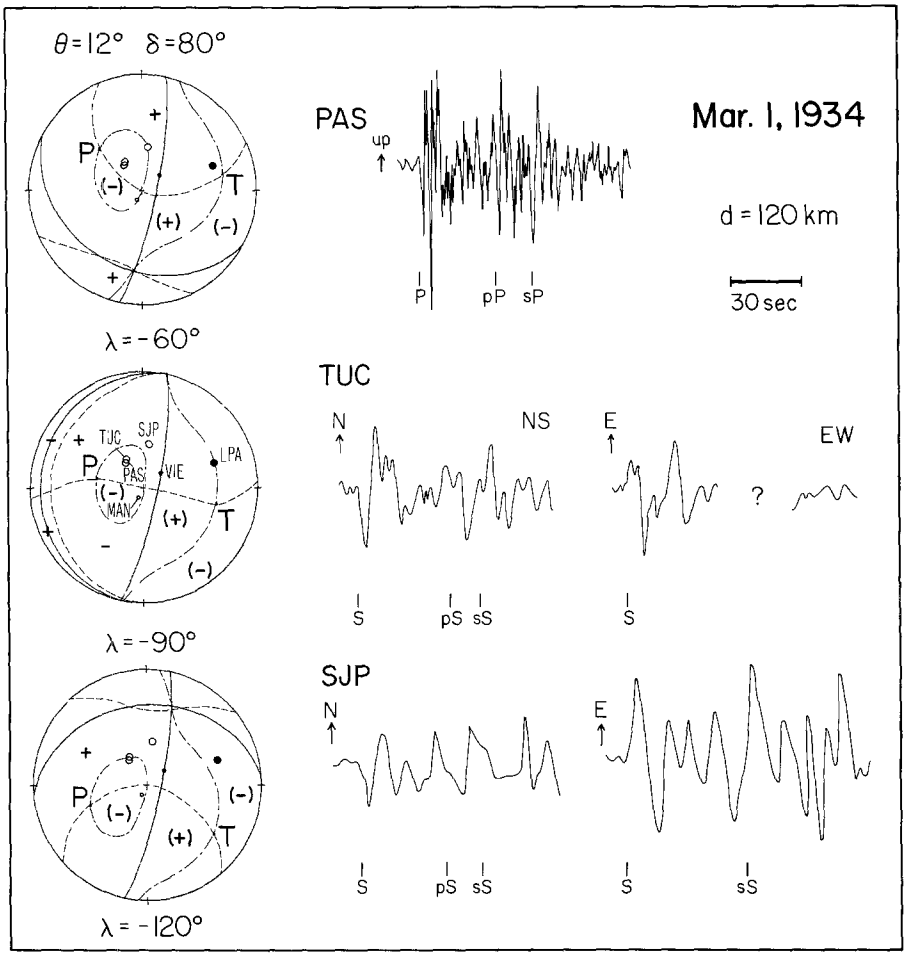

FIG. 5. Seismograms of the 1 March 1934 earthquake. The focal mechanisms are for a steeply dipping normal fault ($\theta = 12°$, $\delta = 80°$) with three different slip angles (λ). The continuous curves are the *P*-wave nodal planes. Short, dash lines indicate the *SH* radiation nodes, where + and − indicate clockwise and counterclockwise rotation around the source, respectively. Long, dash-point lines show the *SV* radiation nodes; + and − are directions away from and toward the source, respectively. The data are consistent with the top focal mechanism.

PAS (1–90) and TUC (1–77). The horizontal instruments at Tucson are Wood-Anderson ($T_0 = 8$ sec), and those at Pasadena are long-period Benioff (1–90). The upper traces in Figure 4 show *P* and rotated *SH* waveforms at these two stations. The *P* and *SH* synthetics (lower traces) constrained the source depth to be 63 km, with a simple 5 sec long source time function. The fault parameters determined using *P*- and *S*-waveform data are $\theta = 350°$, $\delta = 70°$, and $\lambda = -130°$. The focal mechanism in Figure 4 show the radiation nodes for both *P* waves (continuous line) and *SH* waves (dashed line). The average seismic moment obtained from the ratio of observed to synthetic *P* waves is 6.0×10^{26} dyne-cm.

The 1934 earthquake. For this event, the *ISC Bulletin* reports *P*-wave first motion data only for the stations in La Plata (LPA-up), Pasadena (PAS-down), Vienna (VIE-up), and Manila (MAN-down). Fortunately, we could retrieve vertical and horizontal records of various Pasadena instruments from the Caltech seismogram library and also recordings of horizontal 8-sec Wood-Anderson seismographs at

Tucson (TUC) and Wenner-horizontal records ($T_0 = T_g = 10$ sec) at San Juan, Puerto Rico (SJP) from historic seismograms filmed by the U.S. Geological Survey. Figure 5 shows that P waveform recorded at PAS on a Benioff seismograph with $T_0 = 1$ sec and $T_g = 12.5$ sec, and S waves recorded at TUC and SJP by the instruments mentioned above. In spite of the complexity displayed by the P and S waveforms, depth phases can be identified; the expected arrival times of the depth phases shown in Figure 4 are computed for a depth of 120 km which is based on reported pP-P times from nine stations listed in Gutenberg's notepads (Goodstein *et al.*, 1980). This depth is consistent with the sS-S times listed in the *ISC Bulletin* and is considered a good estimate. Although these data are too incomplete to determine the mechanism, we found a mechanism which is consistent with them in the following manner.

At PAS, P-wave first motions are down, east and south. S waves are up, east and south, but are emergent and unclear. At TUC, first motion P data are east and south, and those of S waves are clearly east and south. Unfortunately, a portion of the E-W component after the direct S wave is missing, and it is not possible to time the sS phase. Nevertheless, we could still determine the S-wave polarization. The peak amplitude of the direct S wave on the E-W is similar to those on the N-S component. Since, at TUC, the E-W and N-S components represent approximately SH and SV motions, respectively, we judge the amplitude of the SV component to be comparable to that of SH. We judged the P-wave first motion at TUC to be down, since the horizontal motions are similar to those recorded at PAS. The P-wave first motions at SJP are small and cannot be read, but the S-wave first motions are clearly east and south. The peak amplitude of the E-W component (SH) is twice as large as that of the N-S component (SV). From the SH to SV ratio between TUC and SJP, we consider that SJP is closer to a SV nodal plane than TUC. Note that S-wave polarizations at these three stations are similar. The motion for SH is (+) clockwise rotation around the source and, for SV, it is (−) toward the source. We prefer a steeply dipping ($\delta = 80°$) normal fault, with a strike subparallel to the subduction zone ($\theta = 12°$). This mechanism is consistent with the available P-wave first motions and with focal mechanism solutions of most recent large South American intermediate-depth earthquakes (Figure 1). With this plane fixed, a slip angle $\lambda = -60°$ is consistent with the observed polarization pattern of S waves (Figure 5).

Interpretation and Conclusions

As shown in the previous section, fault plane solutions of the 1949 and 1934 intermediate-depth earthquakes that occurred before the 1960 Chilean earthquake are consistent with steeply dipping normal faults and suggest down-dip tensional stress. Similar steeply dipping normal-fault solutions have been published for two large intermediate-depth events (28 March 1965 and 7 November 1981) down-dip of the rupture areas of the 1971 ($M_W = 7.8$) and the 1985 ($M_W = 8.0$) Valparaiso earthquakes, respectively (Figure 2). Fault parameters for the March 1965 event ($M_W = 7.4$, $d = 72$ km) are $\theta = 350°$, $\delta = 80°$, and $\lambda = -100°$ (Malgrange *et al.*, 1981), and those for the November 1981 event are $\theta = 345°$, $\delta = 86°$, and $\lambda = -93°$ (Dziewonski and Woodhouse, 1983). Thus, large intermediate-depth events which occurred before great underthrust earthquakes in southern Chile are down-dip tensional. In the outer-rise region, the focal mechanism of the 16 October 1981 ($M_S = 7.2$) earthquake ($\theta = 0°$, $\delta = 45°$, $\lambda = 90°$; Christensen and Ruff, 1983), that

occurred before the 1985 Valparaiso earthquake, shows horizontal compression perpendicular to the trench axis. On the other hand, outer-rise events which occurred after the 1960 Chile earthquake on 5 August 1964 ($m_b = 6.1$) and 3 October 1965 ($m_b = 6.0$) indicate horizontal tension perpendicular to the trench axis (Figure 2). The focal mechanisms of the 1964 and 1965 events are $\theta = 181°$, $\delta = 68°$, $\lambda = -56°$, and $\theta = 10°$, $\delta = 70°$, $\lambda = -106°$, respectively (Stauder, 1973). If the 1940 event was in fact an outer-rise event, its relation to the 1960 Chilean earthquake is similar to that of the 1981 outer-rise event (horizontal compression) to the 1985 Valparaiso earthquake. The top diagram in Figure 6 illustrates the state of stress before a large interplate earthquake described above. The bottom diagram illustrates our interpretation of the large down-dip compressional event in May 1971. The large interplate displacement associated with the 1960 great Chilean earthquake changed the stress in the downgoing slab to down-dip compression, and the 1971 event occurred in response to it. It is known that, after large interplate earthquakes, tensional outer-rise events frequently occur (Stauder, 1973). These observations taken together support the notion that the stress propagation in the slab is rather fast; in our case, it is in the order of 10 km/yr.

In conclusion, the interplate boundary is strongly coupled before a major thrust earthquake, and the downgoing slab is under tension at intermediate depths; after the interplate event, the displacement at the boundary induces compressional stress in the down-going slab at intermediate depth and causes down-dip compression events. Outer-rise events, on the other hand, experience the opposite phenomenon; compressional events occur before major underthrusting earthquakes whereas shallow tensional events occur after them (Figure 6). Thus, the spatial and temporal variations of focal mechanisms of outer-rise and intermediate-depth earthquakes may be used to infer the strength of interplate coupling.

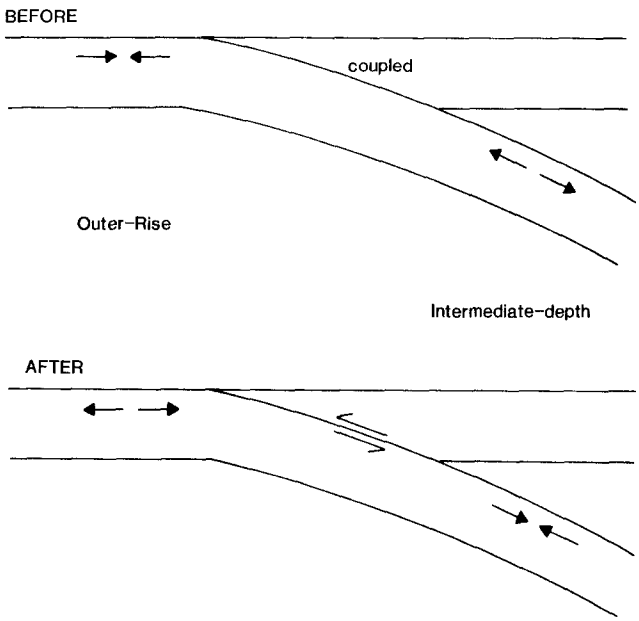

FIG. 6. A schematic diagram showing the intraplate stress before and after a large thrust earthquake for strongly coupled seismic zones.

ACKNOWLEDGMENTS

We thank Larry Ruff for encouragement at an early stage of this project and Thorne Lay for useful discussion. Holly K. Eissler, Steve Grand, Hitoshi Kawakatsu, and Tom Heaton helped us with their critical comments on the manuscript. This research was supported by U.S. Geological Survey Grants 14-08-0001-G1170 and 14-08-0001-G1277, Contribution No. 4343, Division of Geological and Planetary Sciences, California Institute of Technology, Pasadena, California.

REFERENCES

Astiz, L., T. Lay, and H. Kanamori (1984). A global study of intermediate depth earthquake mechanisms, *EOS, Trans. Am. Geophys. Union* **65,** 1015.

Barazangi, M. and B. L. Isacks (1976). Spatial distribution of earthquakes and subduction of the Nazca plate beneath South America, *Geology* **4,** 686–692.

Christensen, C. and L. Ruff (1983). Outer-rise earthquakes and seismic coupling, *Geophys. Res. Letters* **10,** 697–700.

Duda, S. J. (1963). Strain release inthe Circum-Pacific belt, Chile 1960, *J. Geophys. Res.* **68,** 5531–5544.

Dziewonski, A. M. and J. H. Woodhouse (1983). An experiment in the systematic study of global seismicity; centroid moment tensor solutions for 201 moderate and large earthquakes of 1981, *J. Geophys. Res.* **88,** 3247–3271.

Fujita, K. and H. Kanamori (1981). Double seismic zones and stresses of intermediate depth earthquakes, *Geophys. J. R. Astr. Soc.* **66,** 131–156.

Goodstein, J. R., H. Kanamori, and W. Lee (1980). Seismology microfiche publications from the Caltech archives, *Bull. Seism. Soc. Am.* **70,** 657–658.

Gutenberg, B. and C. F. Richter (1954). *Seismicity of the Earth and Associated Phenomena,* Princeton University Press, Princeton, New Jersey, 310 pp.

Hasegawa, A., N. Umino, and A. Takagi (1978). Double-planed structure of the deep seismic zone in the northeastern Japan arc, *Tectonophysics* **47,** 43–58.

Isacks, B. L. and P. Molnar (1971). Distribution of stresses in the descending lithosphere form a global survey of focal-mechanisms solutions of mantle earthquakes, *Rev. Geophys. Space Phys.* **9,** 103–174.

Kanamori, H. and J. J. Cipar (1974). Focal process of the great Chilean earthquake May 22, 1960, *Phys. Earth Planet. Interiors* **9,** 128–136.

Kanamori, H. and G. Stewart (1979). A slow earthquake, *Phys. Earth Planet. Interiors* **18,** 167–175.

Kawakatsu, H. (1986). Double seismic zones: kinematics, *J. Geophys. Res.* **91,** 4811–4825.

Kawakatsu, H. and T. Seno (1983). Triple seismic zone and the regional variation of seismicity along the northern Honshu arc, *J. Geophys. Res.* **88,** 4215–4230.

Kelleher, J. A. (1972). Rupture zones of large South American earthquakes and some predictions, *J. Geophys. Res.* **77,** 2087–2103.

Korrat, I. and R. Madariaga (1986). Rupture of the Valparaiso (Chile) gap from 1971 to 1986 (preprint).

Langston, C. A. and D. V. Helmberger (1975). A procedure for modeling shallow dislocation sources, *Geophys. J. R. Astr. Soc.* **42,** 117–130.

Malgrange, M., A. Deschamps, and R. Madariaga (1981). Thrust and extensional faulting under the Chilean coast: 1965, 1971 Aconcagua earthquakes, *Geophys. J. R. Astr. Soc.* **66,** 313–331.

Plafker, G. and J. C. Savage (1970). Mechanism of the Chilean earthquakes of May 21 and 22, 1960, *Geol. Soc. Am. Bull.* **81,** 1001–1030.

Ruff, L. and H. Kanamori (1983). Seismic coupling and uncoupling at subduction zones, *Tectonophysics* **99,** 99–117.

Seno, T. and B. Pongsawat (1981). A triple structure of seismicity and earthquake mechanisms at the subduction zone off Miyagi Prefecture, northern Honshu, Japan, *Earth Planet. Sci. Letters* **55,** 25–36.

Sleep, N. H. (1979). The double seismic zone in downgoing slabs and the viscosity of the velocity of the atmosphere, *J. Geophys. Res.* **84,** 4565–4571.

Stauder, W. (1973). Mechanism and spatial distribution of Chilean earthquakes with relation of the oceanic plate, *J Geophys. Res.* **78,** 5033–5061.

SEISMOLOGICAL LABORATORY
CALIFORNIA INSTITUTE OF TECHNOLOGY
PASADENA, CALIFORNIA 91125

Manuscript received 13 June 1986